Slow Crack Growth and Fatigue Life prediction of Ceramic Components Subjected to Variable Load History

Final report

Prepared by

Dr. Osama Jadaan
University of Wisconsin-Platteville

Award number: NAG3-2242

Keywords: Reliability, Transient, Weibull, Fatigue, Failure

Abstract. Present capabilities of the NASA CARES/*Life* code include probabilistic life prediction of ceramic components subjected to fast fracture, slow crack growth (stress corrosion), and cyclic fatigue failure modes. Currently, this code has the capability to compute the time-dependent reliability of ceramic structures subjected to simple time-dependent loading. For example, in slow crack growth (SCG) type failure conditions CARES/*Life* can handle the cases of sustained and linearly increasing time-dependent loads, while for cyclic fatigue applications various types of repetitive constant amplitude loads can be accounted for. In real applications applied loads are rarely that simple, but rather vary with time in more complex ways such as, for example, engine start up, shut down, and dynamic and vibrational loads. In addition, when a given component is subjected to transient environmental and or thermal conditions, the material properties also vary with time. The objective of this paper is to demonstrate a methodology capable of predicting the time-dependent reliability of components subjected to transient thermomechanical loads that takes into account the change in material response with time. In this paper, the dominant delayed failure mechanism is assumed to be SCG. This capability has been added to the NASA CARES/*Life* (Ceramic Analysis and Reliability Evaluation of Structures/*Life*) code, which has also been modified to have the ability of interfacing with commercially available FEA codes executed for transient load histories. An example involving a ceramic exhaust valve subjected to combustion cycle loads is presented to demonstrate the viability of this methodology and the CARES/*Life* program.

Introduction

The unique properties of advanced structural ceramics present them as strong candidate materials for many high temperature applications including gasoline, diesel, gas turbine engine components, and aerospace and terrestrial propulsion systems. Attractive properties such as light weight, high strength at elevated temperatures, high stiffness, and corrosion resistance are allowing ceramics to supplant alloys in these demanding applications. The result is lower engine emissions, higher fuel efficiency, and more optimum design.

As improved ceramics emerge for structural applications, the design engineer must be cognizant that the ability of ceramic structures to sustain loads degrades over time due to a variety of effects such as SCG, cyclic fatigue, creep, and oxidation. SCG usually initiates at a preexisting flaw and continues until a critical crack length is reached causing catastrophic failure [1]. Crack extension due to SCG may occur due to interaction between the environment and high stress fields near the crack tip. Cyclic fatigue failure occurs due to repetitive loading that causes premature mechanically assisted failure. In ceramics, this failure takes place due to crack propagation of inherent flaws. Creep rupture, on the other hand, occurs because of bulk damage in the material in the form of void nucleation and coalescence that eventually leads to macrocracks which can then propagate to failure [2]. Hence, it can be seen that in light of the potential use of ceramics in structural applications, life prediction methodologies capable of optimizing material usage and requisite design tools are needed.

Because of the combination of brittleness and the random nature of inherent flaws in ceramic materials, probabilistic analysis and design methodologies are utilized to predict their lifetime. Several integrated design codes such as CARES/*Life* [3], CERAMIC/ERICA [4], and STAU [5] are available and have been demonstrated to be successful in predicting the failure probability for ceramic components subjected to fast fracture and SCG.

Prior to this work the SCG and cyclic fatigue theories in CARES/*Life* were limited to static loading in the case of SCG, and simple constant-amplitude loading in the cyclic fatigue case. In the CERAMIC/ERICA code, the Weibull modulus is assumed to be constant and thus independent of temperature and environment. However, the Weibull modulus for some ceramic materials such as NT551 [6] and alumina [7] has been found to potentially exhibit temperature and stress rate dependence. Prior to this work the CARES/Life code assumed that the material response (parameters) remained constant with time under sustained and fatigue type loading. This means that CARES/Life did not take into account the effects of thermal and environmental changes on the life of a loaded component, although CARES/Life did allow the Weibull modulus to vary with temperature and environment. However, until the methodology described in this paper commenced, CARES/Life assumed the material response at a given location in the component to be constant with time. In practical applications, the majority of applied loads vary with time such as in start up, shut down, dynamic, and vibrational load cases. In addition multiple time varying loads can be applied concurrently. Even if the majority of these applied loads remain static, it takes only one varying load to cause the stress distribution throughout the structure to fluctuate with time.

Previous investigators [8-12] have tackled the issue of transient reliability, where SCG was considered to be the dominant failure mode. Paluszny and Nichols [8] described a methodology to compute the time-dependent reliability of ceramics in SCG failure mode but assumed the Weibull modulus and SCG exponent to remain constant with time. Jakus and Ritter [9] developed a life prediction Eq. in terms of probabilistic parameters for both applied stress and component strength. They assumed that the applied stress varies according to a truncated Gaussian distribution while the strength was modeled using the Weibull distribution. In their analysis, they also assumed the Weibull modulus and the SCG exponent to remain constant with time. More recently Bruckner-Foit and Ziegler [10,11], and Ziegler [12] developed time-dependent reliability formulation for three cases: no SCG, SCG governed by a power law, and SCG governed by a power law with a threshold. In his transient reliability formulation, Ziegler [12] allowed the SCG exponent to vary with time and assumed the Weibull modulus to be constant. Ziegler's approach regarding transient SCG governed by a power law is based on tracking the evolution of crack size as a function of time. The authors of this paper developed a methodology of transient SCG governed by a power law based on an approach of using flaw strength and maintaining compatibility of failure probability between discrete time steps. This methodology allows for the introduction of a variable Weibull modulus as a function of time or temperature. Allowing for a variable Weibull modulus is useful for materials that show R-curve behavior as a function of temperature. In addition, in this paper it is shown how to perform reliability analysis for transient SCG with varying material properties for repeated block loading – a topic not covered in reference [12].

The objective of this paper is to demonstrate this systematic methodology to predict the time-dependent reliability of components subjected to multiple transient thermomechanical loads, taking into account the change in material response with time. This methodology was added to the CARES/Life code as well as the capability to perform this analysis using results generated from the ANSYS finite element analysis program. An example involving a ceramic exhaust valve subjected to combustion cycle loads is presented to demonstrate the viability of this methodology.

Theoretical Development

Transient Reliability With SCG. The derivations that follow will develop the time-dependent probability of survival based on the mode I equivalent stress distribution due to thermomechanical loading at time t_f, transformed to its equivalent stress distribution at time t = 0. Investigations in the area of mode I crack extension [13] have resulted in the following relationship

$$K_{Ieq}(\Psi,t) = \sigma_{Ieq}(\Psi,t)\, Y \sqrt{a(\Psi,t)} \qquad (1)$$

where Y is a function of crack geometry, σ_{Ieq} is the equivalent mode I far field stress normal to a crack, a(t) is the crack length at time t, and Ψ represents a location (x,y,z) within the body and the orientation (α,β) of the crack. In some models, such as the Weibull and principle of independent action (PIA), Ψ represents a location only. The Equations presented in this section are based on the Batdorf theory [20,21]. For the Batdorf theory, $\Psi = (x,y,z,\alpha,\beta)$ for volume flaw analysis and $\Psi = (x,y,\alpha)$ for surface flaw analysis.

The crack growth as a function of the equivalent mode I stress intensity factor can be expressed as

$$\frac{da(\Psi,t)}{dt} = A(t)\, K_{Ieq}^{N(t)}(\Psi,t) \qquad (2)$$

where A(t) and N(t) are time-dependent material constants that depend on the temperature and environment. These constants are described as a function of time in Eq. 2 because in a transient loading analysis the temperature and/or environment can vary with time causing these material constants to change accordingly. From Eqs. 1 and 2 it can be shown that for a given time interval, during which the material parameters are assumed constant, the equivalent transformed stress distribution $\sigma_{Ieq,t_i}(\Psi)$ at the beginning of that time interval $t=t_i$ is related to the degraded strength $\sigma_{Ieq,f} = \sigma_{Ieq}(\Psi, t_f)$ at the end of the time interval $t=t_f$ through the following Eq.:

$$\sigma_{Ieq,t_i}(\Psi) = \left[\frac{\int_{t_i}^{t_f} \sigma_{Ieq}^{N(t)}(\Psi, t)\, dt}{B(t)} + \sigma_{Ieq}^{N(t)-2}(\Psi, t_f) \right]^{\frac{1}{(N(t)-2)}} \tag{3}$$

$$B(t) = \frac{2}{A(t)\, Y^2 K_{IC}^{\,N(t)-2}\, (N(t)-2)} \tag{4}$$

where $\sigma_{Ieq,t} = \sigma_{Ieq}(\Psi, t)$ is the stress distribution during the time interval from t_i to t_f. The material parameters A(t), N(t) and B(t), which can vary over the entire load history, are assumed to be constant during that time interval. The exponent N is dimensionless and B has units stress^2 $\times$ time. The challenge is to solve Eq. 3 for the effective stress distribution $\sigma_{Ieq,0}(\Psi)$ at time $t = 0$ where $\sigma_{Ieq,0}(\Psi)$ is the transformed critical equivalent stress distribution at $t = 0$. Note that Eq. 3 can be used to calculate $\sigma_{Ieq,0}(\Psi)$ directly for the special case when the material parameters N and B are invariant (constant) over the entire load history [14,15]. In this paper we show how to compute $\sigma_{Ieq,0}(\Psi)$ using Eq. 3 for the general case when the material parameters vary with time.

The time-dependent reliability of a ceramic component can be computed assuming a crack density distribution, which is a function of the critical effective stress distribution. For volume analysis, the probability of survival, $P_{SV}(t_f)$, based on the Batdorf model is [3]:

$$P_{SV}(t_f) = \exp\left[-\frac{\bar{k}_{BV}}{4\pi} \int_\Omega \int_V \left[\frac{\sigma_{Ieq,0}(\Psi)}{\sigma_{0V1}} \right]^{m_{V1}} dV d\Omega \right] \tag{5}$$

where $\bar{k}_{BV}$ is the normalized Batdorf crack density coefficient for volume flaws, $\sigma_{Ieq,0}(\Psi)$ is the transformed critical effective stress distribution at t=0 as given in Eq. 3, σ_{oV1} is the Weibull scale parameter at t=0 for volume flaws, m_{V1} is the Weibull modulus at t=0 for volume flaws, and $d\Omega = \sin\alpha\, d\alpha\, d\beta$. $\sigma_{Ieq,0}(\Psi)$ is dependent on the appropriate fracture criterion, crack shape, and time t_f. The term $\bar{k}_{BV}$ is used in the reliability equation for compatibility purposes. It insures that the multiaxial Batdorf theory collapses to the basic uniaxial Weibull model.

It is apparent from Eq. 5 that the key to computing the transient reliability for a structural component is the proper computation of the transformed critical effective stress, $\sigma_{Ieq,0}(\Psi)$, and the knowledge of how the fast fracture and fatigue material parameters (σ_{ov}, m_v, B_v, N_v) vary with time. What follows is a methodology for evaluating $\sigma_{Ieq,0}(\Psi)$ given a fluctuating stress history and material properties.

For a stressed component, the probability of survival is calculated using Eq. 5. The finite element method (FEA) enables discretization of the component into incremental volume elements, V_i corresponding to the ith element. The stress state, temperature, and environment for each element are assumed uniform. In that case, the volume integral is replaced with a volume summation, and Eq. 5 takes the following form:

$$P_{SV}(t_f) = \exp\left[-\sum_{i=1}^{n} \frac{\bar{k}_{BVi} V_i}{4\pi} \left(\int_\Omega \left[\frac{\sigma_{Ieq,0}(\Psi)}{\sigma_{0VI}} \right]^{m_{VI}} d\Omega \right)_i \right] \qquad (6)$$

For enhanced numerical accuracy, CARES/Life evaluates the failure probability at the Gaussian integration points of the element. Using the element integration points subdivides the element into subelements. Hence, V_i in Eq. 6 corresponds to the subelement volume, and n is the total number of subelements.

To take into account the time dependence of loading and material response, we discretize the stress history for each element i into short time steps, Δt_j, during which the stress and material parameters are assumed to remain constant. For a given time step j, the applied equivalent stress in a given element i is given by $\sigma_{Ieq,j}$, the temperature T_j, the scale parameter σ_{ovj}, the Weibull modulus m_{vj}, the fatigue constant B_{vj}, and the fatigue exponent N_{vj}. Note that in Eqs. 5 and 6, the Weibull parameters corresponding to the first load step (initial conditions at t=0), σ_{ovI} and m_{vI}, are used to compute the reliability. This is done to be consistent since the stress history was transformed to the initial conditions at t=0.

The expression for the transformed critical equivalent stress distribution at t = 0 (inert strength), $\sigma_{Ieq,0}(\Psi)$, will be derived next for the first three time steps of a general fluctuating stress history that a given element i experiences. This is done in order to develop a pattern for the inert strength expression that can then be generalized and coded for any time step j.

Time step 1: During this time step Δt_1 and for a given element i, the applied stress is termed $\sigma_{Ieq,1}$, the temperature T_1, the scale parameter σ_{ov1}, the Weibull modulus m_{v1}, the fatigue constant B_{v1}, and the fatigue exponent N_{v1}. The inert strength expression, $(\sigma_{Ieq,0})_i$ for the i[th] element corresponding to the first time step is obtained directly from Eq. 3. In that equation the stress history integral existing in the first term within the brackets is evaluated by setting the stress history $\sigma_{Ieq}(\Psi,t)$ equal to the constant applied equivalent stress during time step 1, $\sigma_{Ieq,1}$, and the failure time $t_f = \Delta t_1$. This means that the integral term in Eq. 3 becomes equal to $\sigma_{Ieq,1}^{N_{V1}} \Delta t_1$. Hence, the inert strength at t=0, $(\sigma_{Ieq,0})_i$ for element i is given by:

$$(\sigma_{Ieq,0})_i = \left[\frac{\sigma_{Ieq,1}^{N_{V1}} \Delta t_1}{B_{V1}} + \sigma_{Ieq,1f}^{N_{V1}-2} \right]_i^{\frac{1}{(N_{V1}-2)}} \qquad (7)$$

The second term in Eq. 7, $\sigma_{Ieq,1f}$, represents the remaining (degraded) strength at the end of time step 1. Since we are interested in computing the failure probability at the end of time step 1, then we assume that the element fails at the end of this time step. Hence, by setting the degraded strength term $\sigma_{Ieq,1f}$ equal to the applied stress $\sigma_{Ieq,1}$ during this time step, we arrive at the probability of failure/survival expression. Therefore, the inert strength expression at time t=0 for the ith element corresponding to a constant loading for the duration of time step 1 becomes:

$$(\sigma_{Ieq,0})_i = \left[\frac{\sigma_{Ieq,1}^{N_{V1}} \Delta t_1}{B_{V1}} + \sigma_{Ieq,1}^{N_{V1}-2} \right]_i^{\frac{1}{(N_{V1}-2)}} \qquad (8)$$

Substituting Eq. 8 into Eq. 6, we obtain the following reliability formula for the entire component at the end of time step 1:

$$P_{SV}(t_1) = \exp\{-\sum_{i=1}^{n} \frac{\bar{k}_{BVi1} V_i}{4\pi} [\int_{\Omega} [(\frac{\sigma_{Ieq,1}}{\sigma_{oV1}})^{N_{V1}-2} + \frac{\sigma_{Ieq,1}^{N_{V1}} \Delta t_1}{\sigma_{oV1}^{N_{V1}-2} B_{V1}}]^{\frac{m_{V1}}{N_{V1}-2}} d\Omega]_i \} \tag{9}$$

Time step 2: During this time step Δt_2 and for a given element i, the applied stress is termed $\sigma_{Ieq,2}$, the temperature T_2, the scale parameter σ_{ov2}, the Weibull modulus m_{v2}, the fatigue constant B_{v2}, and the fatigue exponent N_{v2}. To carry on the reliability analysis to this time step, it is assumed that the initial strength at the beginning of time step 2, $(\sigma_{Ieq,0})_2$, is equal to the remaining strength at the end of time step 1, $\sigma_{Ieq,1f}$. This assumption is valid if the material response does not vary significantly from one step to the next. However, in real applications changes in temperature and environment are the norm. For such cases the remaining strength at the end of one time step does not equal the initial strength of the subsequent time step. Since the crack size does not change from the end of one time step and the beginning of the next one, we can circumvent this problem by computing an equivalent strength at the beginning of a given time step using the remaining strength from the previous time step. This can be done by equating the survival probabilities corresponding to these two cases. Performing the above task results in:

$$\left(\sigma_{Ieq,0}\right)_2 = \left(\frac{\sigma_{0V2}}{\left[\bar{k}_{BV2}\right]^{1/m_{V2}}}\right)\left(\frac{\sigma_{Ieq,1f}}{\left(\frac{\sigma_{oV1}}{\left[\bar{k}_{BV1}\right]^{1/m_{V1}}}\right)}\right)^{\frac{m_{V1}}{m_{V2}}} = \sigma_{0BV2}\left(\frac{\sigma_{Ieq,1f}}{\sigma_{0BV1}}\right)^{\frac{m_{V1}}{m_{V2}}} \tag{10}$$

Eq. (10) provides an expression for the initial strength of time step 2 $(\sigma_{Ieq,0})_2$ as a function of the remaining strength at the end of time step 1 , $\sigma_{Ieq,1f}$. Note that when the Wiebull parameters remain constant Eq. 10 collapses to the basic case where the remaining strength at the end of a given time step is equal to the initial strength of the subsequent step. Also, use of the normalized Batdorf crack density coefficient, $\bar{k}_{BV}$ is essential to normalize the relationship to the uniaxial stress state. The term σ_{0BV} includes the effect of $\bar{k}_{BV}$ and is used henceforth. This is how the methodology described in this paper takes into account the transience in the Wiebull parameters throughout the load history.

The objective now is to obtain an expression for the inert strength at t=0 using the applied constant stresses and material parameters during the first two time steps. This expression can then be substituted back in the reliability Eq. 6 to compute the failure probability at the end of time step 2. This is done through a series of equation manipulations to arrive at the desired goal. From Eq. 3 and for time step 2, the degraded strength at the end of time step 2, $\sigma_{Ieq,2f}$ and the initial strength at the beginning of time step 2 $(\sigma_{Ieq,0})_2$ are related as such:

$$\sigma_{Ieq,2f}^{N_{V2}-2} = \left(\sigma_{Ieq,0}\right)_2^{N_{V2}-2} - \frac{\sigma_{Ieq,2}^{N_{V2}} \Delta t_2}{B_{V2}} \tag{11}$$

Solving Eq. 7 for the degraded strength at the end of time step 1, $\sigma_{Ieq,1f}$, in terms of the inert strength at t=0, $(\sigma_{Ieq,0})_i$, and substituting that term into Eq. 10 yields an expression for the initial strength at time step 2, in terms of the inert strength at time t=0. Taking that expression for $(\sigma_{Ieq,0})_2$ and substituting it into Eq. 11 results in a formula relating the inert strength at t=0 to the degraded strength at the end of time step 2, , $\sigma_{Ieq,2f}$. In order to compute the probability of failure at the end of time step 2, we shall assume that failure occurs when this degraded strength become equal to the applied stress during this time step, $\sigma_{Ieq,2}$. Performing all these mathematical manipulations will ultimately yield the following formulation for the inert strength at t=0 due to a load history made up of two time steps:

$$\left(\sigma_{Ieq,0}\right)_i = [\frac{\sigma_{0BV1}^{N_{V1}-2}}{\sigma_{0BV2}^{\frac{m_{V2}(N_{V1}-2)}{m_{V1}}}} (\sigma_{Ieq,2}^{N_{V2}-2} + \frac{\sigma_{Ieq,2}^{N_{V2}} \Delta t_2}{B_{V2}})^{\frac{m_{V2}(N_{V1}-2)}{m_{V1}(N_{V2}-2)}} + \frac{\sigma_{Ieq,1}^{N_{V1}} \Delta t_1}{B_{V1}}]_i^{\frac{1}{N_{V1}-2}} \tag{12}$$

Eq. 12, in its current form, can lead to decreasing inert strength as time elapses. For example, if the applied stress decreases monotonically with time while the material gets stronger, then Eq. 12 can result in decreasing inert strength as time elapses. This means that when this time dependent inert strength is substituted in Eq. 6, improved reliability can be predicted. This is obviously wrong since a structure's reliability cannot increase with time. Hence, a systematic methodology is necessary to insure that the reliability never increases with time.

The procedure proposed in this work to insure that the reliability never increases with time is based on maximizing the fast fracture term, $\sigma_{Ieq,2}$, in Eq. 12. In this maximization procedure the stress history (all time steps) is transformed using the methodology of Eq. 10 in such a way that the material properties for the entire history remain constant. The material properties for the last time step, k=2, are used as the values to normalize the entire load history with respect to. In other words, for this two time steps loading history, the material properties during time step 1 are transformed to those during time step 2. Obviously the stress during time step 2 remains the same since the material properties during that time step do not change. Hence, the entire load history has the same material properties as time step 2. This transformation is done by computing an equivalent (transformed) stress during time step 1 $\sigma_{Ieq1,2}$, using the material properties of time step 2, that maintains the same probability of failure as the actual applied stress and material properties of time step 1. Hence, The term $\sigma_{Ieq1,2}$ is the transformed stress during time step 1 using the material properties of the last time step, which in this case is 2. This transformation yields the following expression:

$$\sigma_{Ieq1,2} = \sigma_{0BV2} \left(\frac{\sigma_{Ieq,1}}{\sigma_{0BV1}} \right)^{\frac{m_{V1}}{m_{V2}}} \tag{13}$$

Now with the material properties uniform throughout the load history, the fast fracture term in Eq. 12 is set equal to the maximum transformed stress, $\sigma_{Ieq,2,Tmax}$, which is equal to the maximum of either $\sigma_{Ieq1,2}$ or $\sigma_{Ieq,2}$. The second subscript in $\sigma_{Ieq,2,Tmax}$ indicates that the stresses during all time steps have been transformed using the material properties present during the last time step 2, while the last subscript Tmax indicates that the maximum stress during all time steps was selected. This maximization procedure insures that both stress magnitudes and material properties are taken into account when maximizing the fast fracture term in the inert strength formulation.

Substituting the maximum transformed stress into Eq. 12 and subsequently Eq. 12 into Eq. 6, we obtain the following reliability formula for the entire component at the end of time step 2:

$$P_{SV}(t_2) = \exp\{-\sum_{i=1}^{n} \frac{V_i}{4\pi}[\int_{\Omega}[[(\frac{\sigma_{Ieq,2,T\max}}{\sigma_{0BV2}})^{N_{V2}-2} + \frac{\sigma_{Ieq,2}^{N_{V2}}\,\Delta t_2}{\sigma_{0BV2}^{N_{V2}-2}\,B_{v2}}]^{\frac{m_{V2}(N_{V1}-2)}{m_{V1}(N_{V2}-2)}} + \frac{\sigma_{Ieq,1}^{N_{V1}}\,\Delta t_1}{\sigma_{0BV1}^{N_{V1}-2}\,B_{v1}}]^{\frac{m_{V1}}{N_{V1}-2}}\, d\Omega]_i\} \tag{14}$$

Time step 3: During this time step Δt_3 and for a given element i, the applied stress is termed $\sigma_{Ieq,3}$, the temperature T_3, the scale parameter σ_{ov3}, the Weibull modulus m_{v3}, the fatigue constant B_{v3}, and the fatigue exponent N_{v3}.

For time step 3, similar procedure to that performed for time step 2 yields the following expression for the inert strength at t=0 for the ith element at the end of time step 3:

$$\left(\sigma_{Ieq,0}\right)_i = [\frac{\sigma_{0BV1}^{N_{V1}-2}}{\sigma_{0BV2}^{\frac{m_{V2}}{m_{V1}}(N_{V1}-2)}}[\frac{\sigma_{0BV2}^{N_{V2}-2}}{\sigma_{0BV3}^{\frac{m_{V3}}{m_{V2}}(N_{V2}-2)}}(\sigma_{Ieq,3}^{N_{V3}-2} + \frac{\sigma_{Ieq,3}^{N_{V3}}\Delta t_3}{B_{V3}})^{\frac{m_{V3}(N_{V2}-2)}{m_{V2}(N_{V3}-2)}} + \frac{\sigma_{Ieq,2}^{N_{V2}}\Delta t_2}{B_{V2}}]_i^{\frac{m_{V2}(N_{V1}-2)}{m_{V1}(N_{V2}-2)}} + \frac{\sigma_{Ieq,1}^{N_{V1}}\Delta t_1}{B_{V1}}]_i^{\frac{1}{N_{V1}-2}} \tag{15}$$

Using the same maximization procedure described during time step 2, we transform the stresses during time steps 1 and 2 using the material properties of the last time step k=3. Obviously the stress during time step 3 remains the same since the material properties during that time step do not change. Hence, the transformed stresses during time steps 1 and 2 are given by the terms $\sigma_{Ieq1,3}$ and $\sigma_{Ieq2,3}$. Now with the material properties uniform throughout the load history, the fast fracture term in Eq. 15 is set equal to the maximum transformed stress, $\sigma_{Ieq,3,Tmax}$, which is equal to the maximum of $\sigma_{Ieq1,3}$, $\sigma_{Ieq2,3}$ or $\sigma_{Ieq,3}$. The second subscript in $\sigma_{Ieq,3,Tmax}$ indicates that all stresses have been transformed using the material properties present during the last time step 3, while the last subscript Tmax indicates that the maximum stress during all time steps was selected.

Substituting the maximum transformed stress for the fast fracture term in Eq. 15 and subsequently Eq. 15 into Eq. 6, we obtain the following reliability formula for the entire component at the end of time step 3:

$$P_{SV}(t_3) = \exp\{-\sum_{i=1}^{n} \frac{V_i}{4\pi}[\int_{\Omega}[[[(\frac{\sigma_{Ieq,3,T\max}}{\sigma_{0BV3}})^{N_{V3}-2} + \frac{\sigma_{Ieq,3}^{N_{V3}}\,\Delta t_3}{\sigma_{0BV3}^{N_{V3}-2}\,B_{V3}}]^{\frac{m_{V3}(N_{V2}-2)}{m_{V2}(N_{V3}-2)}} + \frac{\sigma_{Ieq,2}^{N_{V2}}\,\Delta t_2}{\sigma_{0BV2}^{N_{V2}-2}\,B_{V2}}]^{\frac{m_{V2}(N_{V1}-2)}{m_{V1}(N_{V2}-2)}} + \frac{\sigma_{Ieq,1}^{N_{V1}}\,\Delta t_1}{\sigma_{0BV1}^{N_{V1}-2}\,B_{V1}}]^{\frac{m_{V1}}{N_{V1}-2}}\, d\Omega]_i\} \tag{16}$$

Comparing the reliability Eqs. 9, 14, and 16 at the end of the first three time steps, a clear pattern emerges. This pattern is used for coding purposes. It can be seen from these functions that the transient reliability equation, when taking into account the change in material response, is an ever-expanding function, which adds nested terms as more time steps are considered. By inductive argument then for *k* time steps

$$P_{SV}(t_k) = \exp\{-\sum_{i=1}^{n} \frac{V_i}{4\pi}[\int_{\Omega}[\ldots[\;[\;(\frac{\sigma_{Ieq,k,T\max}}{\sigma_{0BVk}})^{N_{Vk}-2} + \frac{\sigma_{Ieq,k}^{N_{Vk}}\Delta t_k}{\sigma_{0BVk}^{N_{Vk}-2}B_{Vk}}]_k^{\frac{m_{Vk}(N_{Vj}-2)}{m_{Vj}(N_{Vk}-2)}} + \frac{\sigma_{Ieq,j}^{N_{Vj}}\Delta t_j}{\sigma_{0BVj}^{N_{Vj}-2}B_{Vj}}]_j^{\frac{m_{Vj}(N_{Vi}-2)}{m_{Vi}(N_{Vj}-2)}} + \\ \ldots. + \frac{\sigma_{Ieq,1}^{N_{V1}}\Delta t_1}{\sigma_{0BV1}^{N_{V1}-2}B_{V1}}]_1^{\frac{m_{V1}}{N_{V1}-2}} d\Omega]_i\} \tag{17}$$

where k is the last time step, j=*k*-1, i=*k*-2, and so on. This is why the derivation for the inert strength and reliability functions was done in a gradual manner by considering each time step separately, rather than attempting to derive a general expression for an arbitrary k^{th} time step.

It is apparent from Eq. 17 that the transient reliability is dependent on the load and thermal/environmental history. The dependence on the thermal/environmental load history comes from the sequential order of the exponential term $m_{vk}(N_{vj}-2)/m_{vj}(N_{vk}-2)$. When the material parameters m and N remain constant with time (temperature and environment do not vary with time), then the exponential terms become equal to 1. Under such circumstances the transient reliability becomes independent of both load and thermal/environmental history. For materials like ceramics where little or no plasticity takes place, load history independence when the material properties do not vary with time is anticipated.

In many engineering applications, structural components are subjected to repeated block loading. Fig. 1 shows a schematic diagram of such a loading history where a component is subjected to Z number of repeated load blocks. Such repeated block loading and its effect on damaging the ceramic structural component can be incorporated into the transient reliability analysis.

Eq. 17 is the general formulation for obtaining the transient reliability of components subjected to varying thermomechanical loading. However because this equation is numerically intensive when many time steps are involved, it is desirable to take advantage of the repeated nature of block loading to develop a simpler and numerically less demanding equation. In general, as was stated earlier, the transient reliability is load and temperature/environment dependent. However, for cases when the reliability dependence on thermal/environmental loading is weak or nonexistent (such as when the temperature and environment do not vary significantly with time) then Eq. 17 simplifies to the following formulation for a component subjected to Z similar load blocks:

$$P_{SV}(t_k) = \exp\{-\sum_{i=1}^{n} \frac{V_i}{4\pi}[\int_{\Omega}[\ldots[\,[(\frac{\sigma_{Ieq,k,T\max}}{\sigma_{0BVk}})^{N_{Vk}-2} + \frac{\sigma_{Ieq,k}^{N_{Vk}}Z\Delta t_k}{\sigma_{0BVk}^{N_{Vk}-2}B_{Vk}}]_k^{\frac{m_{Vk}(N_{Vj}-2)}{m_{Vj}(N_{Vk}-2)}} + \frac{\sigma_{Ieq,j}^{N_{Vj}}Z\Delta t_j}{\sigma_{0BVj}^{N_{vj}-2}B_{Vj}}]_j^{\frac{m_{Vj}(N_{Vi}-2)}{m_{Vi}(N_{Vj}-2)}} + \\ \ldots + \frac{\sigma_{Ieq,1}^{N_{V1}}Z\Delta t_1}{\sigma_{0BV1}^{N_{V1}-2}B_{V1}}]_1^{\frac{m_{V1}}{N_{V1}-2}} d\Omega]_i\} \tag{18}$$

The reason Eq. 17 collapses to Eq. 18 when the reliability is assumed or approximated to be load and temperature independent, is that all Z similar time steps can be joined together to form one large time step with duration $Z\Delta t_i$ where i represents a given time step within a load block. By performing this task for all time steps, Eq. 17 can directly be simplified to Eq. 18. It is only necessary to scan one load block when using Eq. 18 to predict the transient reliability for a component subjected to many load blocks. Again Eq. 18 should be used under the assumption that the reliability is load and thermal/environmental history independent or if the user is interested in a quick first approximation for the reliability.

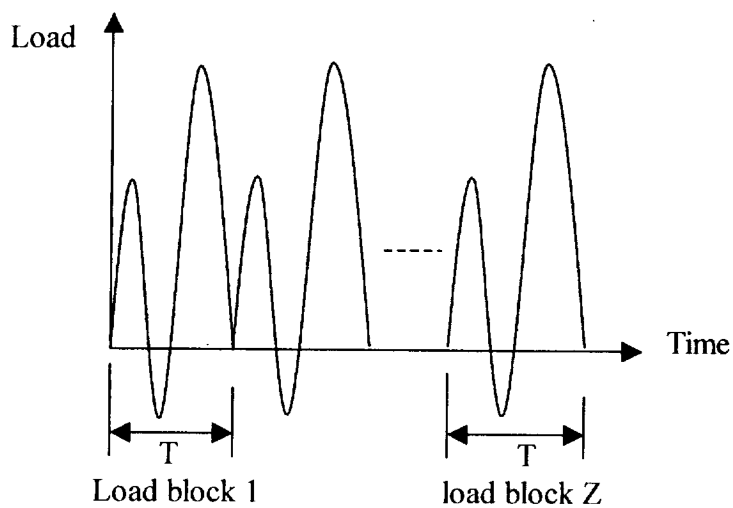

Fig. 1: Schematic diagram of repeated block loading. Number of repeated blocks = Z.

At this point a brief discussion regarding the variability of the Weibull modulus is in order. The assumption that the Weibull modulus can vary with time and temperature is reasonable given that no new flaws are being generated, and that only reversible changes in the physics of crack growth occur. Allowing for a variable Weibull modulus is useful for materials that show R-curve behavior as a function of temperature. R-curve behavior can be strongly temperature dependent, and just as importantly, be modeled as reversible under certain circumstances. Transformation toughened materials show temperature dependent (and reversible) R-curve behavior through changes in the materials crystalline structure with temperature. Mechanically toughened materials show R-curve behavior through grain bridging near crack tips. CARES/Life as described herein models Weibull modulus variability in a phenomenological manner. This means, for example, that CARES/Life does not explicitly account for progressive R-curve degradation from cyclic loading for mechanically toughed materials. Therefore, it is important to ascertain if changing Weibull modulus is due to reversible or irreversible changes in the material. An example of an irreversible change is high temperature corrosion, where new flaw generation on the material surface may result (also oxidation, erosion, and impact damage are irreversible processes). In the example problem shown later, the silicon carbide (SIC) material shows a change in Weibull modulus with temperature, which is possibly associated with flaw healing and/or new flaw generation (an irreversible process). Since the temperature gradient for the example component changes very little over time, the Weibull modulus consequently does not vary over time for a given location in the component body. Hence, use of the temperature dependent Weibull parameters is appropriate in this case (because it is not modeled as a reversible quantity). Had the thermal profile significantly varied over the loading cycle, then using a strictly temperature varying Weibull modulus would likely not be appropriate.

In a study conducted by Andrews et al. [22], NT 551 diesel exhaust ceramic valves were tested under fast fracture conditions at room temperature. Two sets of valves were examined. The first set contained 25 as-received (pristine) valves. Of these 25 valves, 15 were machined transverse to the axis of symmetry while 10 were machined longitudinally. The dominant mode of failure for the transversely machined valves was surface-induced from machining damage, while the dominant mode of failure for the longitudinally machined valves was volume induced from compositional inhomogeneities. The uncensored Weibull modulus for the transversely machined valves was 8.3, while that for the longitudinally machined valves was 15.3. The second set contained 15 engine-tested valves which were loaded to failure in order to examine their retained strength. These valves consisted of 7 longitudinally machined valves and 8 transversely machined valves. The transversely machined valves had been engine tested for 1000 hours while the longitudinally machined valves had been engine tested for 166 hours. The dominant mode of failure for both valve-machining orientations was found to be volume induced. The uncensored retained strength Weibull modulus of the engine tested transversely machined valves was 3.9, while that for the longitudinally machined valves was 6.9.

As stated by Andrews et al [22], the results of the fractographic analysis stated above indicates that the mode of failure for the longitudinally machined valves remained the same while the mode of failure changed from surface to volume from the transversely machined valves. In addition, more than 50 % reduction in the uncensored Weibull modulus between the as received and the engine-tested valves for both machining conditions transpired. These results indicate that under transient loading not only can the Weibull modulus vary with time, but also the mode of failure itself. The change in the Weibull modulus may be a result of the changing flaw population (as time elapses) and/or mode of failure.

With the methodology developed herein, it is possible to model the Weibull modulus as an irreversible material property that varies with time and/or temperature. For example, the Weibull modulus can be modeled as a monotonically increasing (or decreasing) function with time, cyclic frequency, or temperature.

All the derivations shown above were performed based on the assumption that volume flaws control failure. When surface flaws dominate the failure process, similar equations integrated over the surface area are used to compute the transient reliability.

Transient Reliability Without SCG: In the case where a component is manufactured using a material resistant to SCG and thus does not degrade with time, the transient reliability formulation becomes much simpler. Since the inherent flaws do not grow with time, we simply need to track the applied stress history and compute the corresponding failure probability as a function of time.

This analysis is identical to the fast-fracture analysis with the exception that it has to be done, as many times as there are time steps. Hence, a given stress history is broken into short time steps during which the stress, temperature, and environment are assumed constant. The reliability, $P_{sv}(t_j)$, is then calculated at the end of each time step, j, using the following Eq.:

$$P_{SV}(t_j) = \exp\left[-\sum_{i=1}^{n} \frac{(\bar{k}_{BV\,j})_i\, V_i}{4\pi} \left(\int_{\Omega} \left(\frac{\sigma_{Ieq,j}}{\sigma_{0V,j}} \right)^{m_{Vj}} d\Omega \right)_i \right] \tag{19}$$

where $(\sigma_{Ieq,j})_i$ is the applied effective stress in the ith element during the jth time interval, while the parameters $(k_{BVj})_i$, $(\sigma_{ovj})_i$, and $(m_{vj})_i$ represent the material properties for the same element and time interval.

It is apparent from Eq. 19 that the reliability increases as the applied stress decreases. While this is true for instantaneous fast fracture loading, prudence should be exercised when applying that equation to time dependent loading when no damage occurs. For example, if a given component is subjected to decreased loading, then Eq. 19 will numerically predict increased reliability for that component as time elapses. However, a component's reliability cannot improve with time. Hence, for cases where the loading eases at a given time step j+1 (the computed reliability increases) the reliability is set equal to that at the previous time step. In other words decreased loading does not result in increased reliability but keeps it constant. In the case of repeated block loading when the material does not degrade with time, the transient reliability analysis needs to be conducted for only one load block. This is because the reliability vs. time curves are identical for all load blocks since no damage takes place.

Numerical Example

To demonstrate the methodology described above, an example involving a ceramic exhaust valve was selected. The design and strength evaluation of this ceramic valve, which is to be used in heavy duty diesel engines, was conducted at Oak Ridge National Laboratory by Corum et al. [17] as part of a Cooperative Research and Development Agreement (CRADA) between Detroit Diesel Corporation and Lockheed Martin Energy Systems, Inc., on behalf of the US Department of Energy. The motivation for that project was that the replacement of the metal exhaust valves with ceramic valves would prolong valve life and permit higher operating temperatures [17]. In this example, we obtained the final valve design geometry and applied loading during a typical engine cycle from Corum in the form of ANSYS input files and from reference [17].
The valves were made of Norton SiALON NT-451 material. Static and fatigue tests were conducted only at room temperature since for this material the strength drops only by 8% going from room temperature to 704 °C (1300 °F), the approximate mean operating temperature of the valve head [17].

Since the valve is subjected to repeated loading for many cycles, cyclic fatigue is expected to be the actual dominant mode for delayed failure. However, in this paper the valve was used to demonstrate a transient reliability analysis with SCG as the dominant failure mode. Fig. 2 represents one pressure cycle applied to the valve face. The repeated nature of pressure cycling applied to the valve face is used in this example to demonstrate the block loading capability described previously in Eq. 18.

Since reference [17] did not include SCG data for NT451, a different valve material was assumed for the purpose of this example. The material selected is a sintered alpha silicon carbide (SASC), which was tested by Jadaan [18] and shelleman [19]. Table 1 contains a summary of the Weibull and SCG parameters for this material at two temperatures. These parameters were used to compute the reliability for the valve in this paper.

The actual mean thermal profile within the valve during a combustion cycle was altered to correspond to the SASC material used in this example. This valve's temperature distribution was hypothetically increased in order to get the material into the temperature range where SCG takes place.

Therefore, in this example only the valve geometry and loading history were kept authentic as reported in reference [17], while the material and thermal profile were altered.

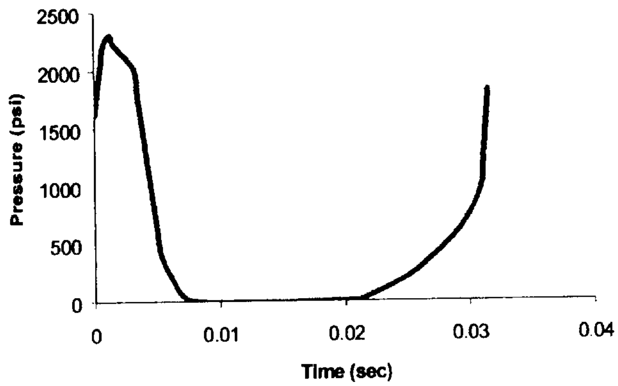

Fig. 2: Pressure variation applied to the face of a ceramic valve during a typical engine combustion cycle.

Table 1: SASC fast fracture and SCG material properties.

Temp(^{0}C)	Weibull modulus (m)	Scale parameter (σ_{0V}) (MPa.mm$^{3/m}$)	Average strength (MPa)	SCG exponent N	SCG parameter B (MPa^2.sec)
25	14.4	300	232		
1200	9.6	378	245	20	4336
1300	6.5	721	248	20	4074

The loading history applied to the valve during a combustion cycle was obtained from reference [17]. Fig. 2 shows the pressure variation as a function of time during a typical combustion cycle. The pressure is applied to the valve's face and other exposed surfaces within the cylinder. The maximum attained pressure during the combustion cycle was estimated to be 15.85 MPa (2300 psi) [17]. A 445 N (100 lb) force due to spring pre-load is applied to the valve stem when it is in the open position. At the moment the valve closes an impact force of 1335 N (300 lb) is applied to the valve stem. In addition, thermal stresses due to the temperature distribution in the valve are superposed to the mechanical stresses.

Fig. 3 shows the assumed mean thermal profile in the valve. Steady-state thermal analysis using ANSYS FEA code was conducted to compute these temperatures. This figure shows that the temperature is maximum near the valve face and decays towards the valve seat and stem.

The transient reliability analysis based on the methodology described above was conducted by dividing the load history into 29 time steps, during each the load was assumed constant. The loads corresponding to these time steps were modeled into ANSYS FEA code, which yielded the stress results for these 29 time steps (stress history). Fig. 4 highlights the first principal thermomechanical stress distribution in the valve at the moment of maximum applied pressure (most critical point of the load history). From the figure it is apparent that the maximum stress location is at the valve radius, which is in agreement with the FEA results of Corum et al. [17]. Initially the failure probabilities were computed using these stresses (Fig. 4), which correspond to the actual loading as shown in Fig. 2. This stress state resulted in very low failure probabilities due to the high material strength compared to the actual applied loading. In order to boost the failure probabilities for this example the valve stresses were increased by 20%. Hence, in this example the failure probabilities were computed by increasing the stress distribution shown in Fig. 4 by 20%.

The valve's stress history and other relevant terms (temperature, volume, material properties, element number, etc.) were subsequently read into CARES/Life. The failure probability as a function of time (number of cycles converted to time since 1 cycle = 0.0315 seconds) was then computed using the transient reliability analysis described previously. Fig. 5 shows a risk of rupture plot for the valve. Fig. 6 shows the transient reliability curve as a function of time (load cycles). As can be seen from that figure, the probability of failure increases as time elapses.

A static reliability analysis using the maximum load level (load step 6) during the load cycle was performed and compared to the transient reliability analysis based on the actual loading. Fig. 6 contains the results of this analysis. As can be seen from this figure, the static loading at the maximum level yielded significantly higher failure probabilities (more conservative) compared to the transient loading case. For example after 1 million seconds, the failure probability based on transient loading analysis is 17.8% compared to 30.7% based on maximum static loading analysis. This means that for the valve example, assuming static loading at the maximum load level for 1 million seconds, almost doubles the failure probability based on the actual transient loading for 1 million seconds. These results, showing higher failure probabilities for the static loading compared to the transient loading, make sense since the valve is not even loaded for some time during each cycle.

Transient analysis can be time consuming since it involves numerically intensive computations. However, depending on the structure and loading, making the assumption that static reliability analysis at the maximum load level can produce close results using the actual loading is not always accurate. Such static analysis can lead to over-designed structures. It is up to the engineer to decide whether a transient analysis is worth performing for the sake of achieving a more optimum design.

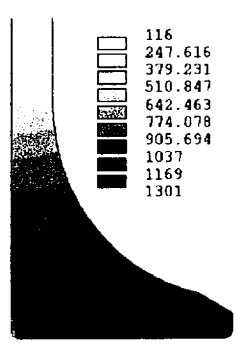

Fig. 3: Mean thermal profile in the ceramic valve. Temperature in °C.

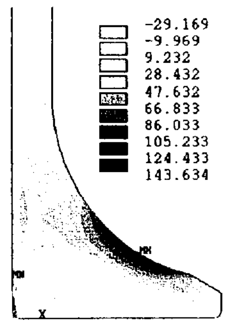

Fig. 4: First principal stress distribution in the valve at the moment of maximum applied pressure. Stress in MPa.

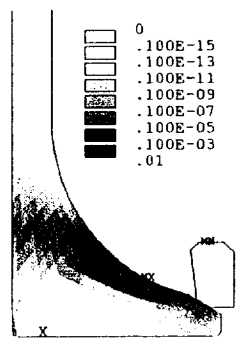

Fig. 5: Risk of rupture map for the ceramic valve.

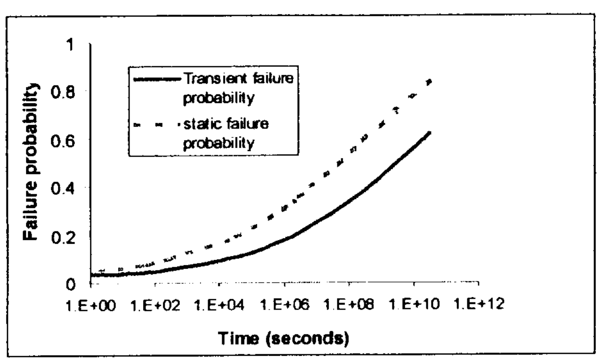

Fig. 6: Transient and static Probability of failure as a function of time for the ceramic valve.

Conclusions

A methodology for computing the transient reliability in ceramic components subjected to fluctuating thermomechanical loading was developed. For this effort it is assumed that delayed failure is controlled by the SCG failure mechanism. In this methodology varying material response, whether due to temperature or environmental changes, can be taken into account. Repeated Block loading was also embedded into the analysis. The theory advanced in this paper represents a more generalized formulation of that proposed by Ziegler [12] since it incorporates a variable Weibull modulus. The fact that the transient reliability Eq.s shown in this paper were derived in a different manner as those derived by Ziegler, yet fundamentally concur with each other, adds more confidence in the accuracy of the methodology proposed by both parties. This methodology was programmed into NASA's CARES/Life code. An example demonstrating the viability of the analysis was presented. From this example it was demonstrated that substantial differences between the reliability assuming constant maximum loading and that based on actual transient loading exist. Designing based on static (constant) loading at the maximum level can lead to conservative but over-designed components.

References

[1] S. M. Wiederhorn, "Subcritical Crack Growth in Ceramics," Fracture Mechanics of Ceramics, edited by R. C. Bradt, D. P. H. Hasselman, and F. F. Lange, Vol. 2, Plenum Press, New York, NY (1974), p. 613-646.

[2] G. Grathwohl, "Regimes of Creep and Slow Crack Growth in High-Temperature Rupture of Hot-Pressed Silicon Nitride," Deformation of Ceramics II, edited by R. E. Tressler, and R. C. Bradt, Plenum Press, New York, NY (1984), p. 573-586.

[3] N. N. Nemeth, L. P. Powers, L. A. Janosik, and J. P. Gyekenyesi, "Ceramics Analysis and Reliability Evaluation of Structures Life Prediction Program, Users and Programmers Manual," NASA Glenn Research Center, Life Prediction Branch (1993).

[4] A. D. Peralta, D. C. Wu, P. J. Brehm, J. C. Cuccio, and M. N. Menon, "Strength Prediction of Ceramic Components Under Complex Stress States," Allied Signal Document No. 31-12637 (1995).

[5] A. Heger, Ph. D. Thesis, Karlsruhe University (1991), (in German).

[6] A. Wereszczak, K. Breder, M. Andrews, Kirkland, T., and Ferber, M., "Strength Distribution Changes in a Silicon Nitride as a Function of Stressing Rate and Temperature," ASME paper number 98-GT-527, International Gas Turbine and Aeroengine Congress and Exhibition, Stockholm, Sweden (1998).

[7] J. E. Ritter, Jr., and Humenik, Journal of Materials Science, vol. 14 (1979), p. 626-632.

[8] A. Paluszny, and P. F. Nicholls, "Predicting Time-Dependent Reliability of Ceramic Rotors," Ceramics for High Performance Applications-II, edited by J. Burke, E. Lenoe, and N. Katz, Brook Hill, Chesnut Hill, Massachuestts (1978).

[9] K. Jakus, and J. Ritter, "Lifetime Prediction for Ceramics Under Random Loads," Res Mechanica, vol. 2 (1981), p. 39-52.

[10] A. Bruckner-Foit, and C. Ziegler, "Design Reliability and Lifetime Prediction of Ceramics," Ceramics:Getting into the 2000's, edited by P. Vincenzini (1999).

[11] A. Bruckner-Foit, and C. Ziegler, "Time-Dependent Reliability of Ceramic Components Subjected to High-Temperature Loading in a Corrosive Environment," ASME paper number 99-GT-233, International Gas Turbine and Aeroengine Congress and Exhibition, Indianapolis, Indiana (1999).

[12] C. Ziegler, Bewertung der Zuverlassigkeit Keramischer Komponenten bei zeitlich veranderlichen Spannungen und bei Hochtemperaturbelastung, Ph.D. Thesis (in German), Karlsruhe University (1998).

[13] P. Paris, and G. Sih, "Stress Analysis of Cracks," ASTM STP 381 (1965), p. 30-83.

[14] T. Thiemeier, Lebensdauervorhersage fur Keramische Bauteile Unter Mehrachsiger Beanspruchung, Ph.D. dissertation (in German), University of Karlsruhe (1989).

[15] G. Sturmer, A. Shulz, and S. Wittig, "Lifetime Prediction for Gas Turbine Components," ASME Preprint 91-GT-96 (1991).

[16] W. Weibull, "The phenomenon of Rupture in Solids," Ingeniors Ventenskaps Akademien Handlinger, No. 153 (1939).

[17] J. Corum, R. Battiste, R. Gwaltney, and C. Luttrell, Design Analysis and Testing of Ceramic Exhaust Valve for Heavy Duty Diesel Engine, ORNL/TM-13253, prepared by Oak Ridge National Laboratory (1996).

[18] O. Jadaan, Fast Fracture and Lifetime Prediction of Ceramic Tubular Components, Ph.D. thesis, The Pennsylvania State University (1990).

[19] D. Shelleman, Test Methodology For Tubular Ceramics (Fast Fracture Strength Study), Ph.D. thesis, The Pennsylvania State University (1991).

[20] S. B. Batdorf, and J. G. Crose, "A Statistical Theory for the Fracture of Brittle Structures Subjected to Nonuniform Polyaxial Stresses," Journal of Applied Mechanics, Vol. 41, No. 2 (1974), p. 459-464.

[21] S. B. Batdorf, and H. L. Heinisch, Jr., "Weakest Link Theory Reformulated for Arbitrary Fracture Criterion," Journal of the American Ceramic Society, Vol. 61, No. 7-8 (1978), P. 355-358.

[22] M. J. Andrews, A. A. Wereszczak, T. P. Kirkland, and K. Breder, Strength and Fatigue of NT551 Silicon Nitride and NT 551 Diesel Exhaust Valves, Report prepared by Oak Ridge National Laboratoy for the US Department of Energy (2000).